JOURNAL OF MATERIALS SCIENCE 28 (1993) 5050–5055

Low-temperature synthesis of chemically homogeneous lead zirconate titanate (PZT) powders by a semi-wet method

A. P. SINGH, S. K. MISHRA, D. PANDEY
School of Materials Science and Technology, Institute of Technology, Banaras Hindu University, Varanasi-221005, India

CH. D. PRASAD, R. LAL
Naval Chemical and Metallurgical Laboratory, Naval Dockyard, Bombay-400023, India

A semi-wet procedure for the synthesis of single-phase $Pb(Zr_xTi_{1-x})O_3$ powders at 600 °C is described. The ultrafine powders so obtained do not exhibit tetragonal/rhombohedral distortions until they are sintered at higher temperatures. The morphotropic phase boundary (MPB) for these powders, which are chemically homogeneous, lies between $x = 0.52$ and 0.53. For $x = 0.525$, the rhombohedral and tetragonal phases coexist.

1. Introduction

Lead zirconate titanate, $PbZr_xTi_{1-x}O_3$ (PZT), ceramics are extensively used as electromechanical transducer materials. The electromechanical response of these ceramics is maximum [1] when x corresponds to the composition of the morphotropic phase boundary (MPB) which separates the tetragonal (T) and rhombohedral (R) phases towards Ti-rich and Zr-rich sides, respectively. The precise determination of the MPB composition range, which is believed [2] to be quite narrow, has, therefore, attracted immense interest. Thermodynamically, the MPB is expected to be a two-phase region over which the rhombohedral and tetragonal phases should coexist. However, the coexistence of the two phases can also be due to compositional fluctuations at the Zr/Ti site because of the sensitivity of the crystal structure (tetragonal/rhombohedral) to small variations in x around the MPB composition. To determine the true MPB composition range, it is imperative to synthesize PZT powders free from compositional fluctuations at the Zr/Ti site.

Conventionally, PZT powders are prepared by solid-state thermochemical reactions in a mixture of PbO, ZrO_2 and TiO_2 particles. In this dry route of synthesis, unit-cell-level uniform distribution of Zr/Ti ions at the B site of the ABO_3 perovskite structure cannot be ensured because the reaction takes place in several steps, with $PbTiO_3$ formation at an early stage of the reaction [1, 3]. The conversion of the intermediate phases into PZT involves long-range diffusion leading to frozen-in compositional fluctuations. Further, the completion of the reaction by long-range diffusion also requires higher temperatures (> 1000 °C). A lower calcination temperature, on the other hand, is always desirable since it yields finer powders with better reactivity leading to higher sintered densities at lower firing temperatures.

In the present work, compositionally homogeneous PZT powders were prepared at 600 °C by a semi-wet route involving a solid-state thermochemical reaction between $PbCO_3$ and $(Zr_xTi_{1-x})O_2$ solid-solution precursors. The importance of solid-solution precursors in the semi-wet synthesis of compositionally homogeneous powders in short calcination durations, and in certain systems at lower calcination temperatures, has been pointed out by Tiwari *et al.* [4] and Pandey et al. [5, 6] for $Ba_{1-x}Ca_xTiO_3$ and $Bi_{1.6}Pb_{0.4}Sr_2Ca_2Cu_3O_y$ oxides. The $(Zr_xTi_{1-x})O_2$ precursors in the present work were obtained by thermal decomposition of $Zr_xTi_{1-x}(OH)_4$ prepared by a coprecipitation method. X-ray diffraction (XRD) of the $(Zr_xTi_{1-x})O_2$ so obtained has revealed these precursors to be solid solutions. As a result of solid-solution formation, atomic-level homogeneous distribution of Zirconium and Titanium has already been achieved. This will ensure a uniform supply of Zirconium and Titanium ions during the solid-state thermochemical reaction with $PbCO_3$/PbO leading to the direct formation of PZT powders of the desired Zr/Ti ratio. Since $(Zr_xTi_{1-x})O_2$ is very refractory while PbO is quite mobile due to its low melting point, PZT may be formed at much lower temperatures by the diffusion of mobile PbO into the $(Zr_xTi_{1-x})O_2$ matrix.

From a combined differential thermal analysis/thermogravimetric analysis (DTA/TGA) and XRD study of this mixture, it is shown that single-phase PZT powders can be prepared at as low a temperature as 600 °C within a short duration, 6 h, using the proposed semi-wet route. The conventional dry route, using $PbCO_3$, ZrO_2 and TiO_2 powders, is found to yield a mixture of PbO, ZrO_2, TiO_2, $PbTiO_3$ and $PbZrO_3$ and no PZT at all even after calcining at 700 °C for 6 h. The PZT powders synthesized by the semi-wet route are of sub-micrometre size and as such

0022–2461 © *1993 Chapman & Hall*

do not display the characteristic tetragonal/rhombohedral splittings on the X-ray powder diffractograms. On sintering these powders above 1000 °C, the characteristic symmetries become discernible. The tetragonal structure is shown to persist up to $x = 0.52$ while at $x = 0.53$ the structure is found to be rhombohedral. Both, tetragonal and rhombohedral phases are confirmed to be free from compositional fluctuations by X-ray-line-broadening analysis. Despite the absence of compositional fluctuations, coexistence of tetragonal and rhombohedral phases was observed for $x = 0.525$, which is within the MPB range.

It may be mentioned that Kakegawa *et al.* [2, 7] have also prepared compositionally homogeneous powders using $(Zr_xTi_{1-x})(OH)_4$ precursors. However, these workers did not: (i) look for the solid-solution formation of $(Zr_xTi_{1-x})O_2$; (ii) optimise the lowest possible calcination temperature (instead a temperature of 1200 °C was used for PZT formation) to get fine, reactive powders; and (iii) get evidence for the coexistence of rhombohedral and tetragonal phases for the MPB composition in compositionally homogeneous PZT powders.

2. Experimental procedure

Following Kakegawa *et al.* [2], Zr and Ti were coprecipitated as hydroxides from their corresponding nitrate solutions using ammonium hydroxide as a precipitating agent. The $(Zr_xTi_{1-x})(OH)_4$ (where $x = 0.515$, 0.520, 0.525 and 0.530) powders are amorphous and agglomerated. The hydroxides were decomposed into the corresponding oxides by heating at 900 °C for 3 h. A further increase in the heat-treatment time at 900 °C did not lead to any additional weight loss, confirming complete decomposition of the precursor hydroxides into oxides. These oxide precursors were mixed with $PbCO_3$ in stoichiometric proportions. These mixtures were then ball milled for 6 h in zirconia jars with zirconia balls using acetone as the mixing medium. DTA/TGA was carried out on a mixture with $x = 0.525$ using a simultaneous thermal analyser (model 409, Netzsch, Germany), at a heating rate of 5 °C min^{-1}. On the basis of the DTA and TGA results, ball-milled powders for $x = 0.525$ were calcined at 500, 600 and 700 °C for 6, 6 and 2 h, respectively. The formation of PZT in these calcined powders was checked by XRD using a 12 kW rotating-anode X-ray diffractometer (model Rotaflex, M/s Rigaku, Japan) operating at 120 mA and 50 kV at a scan speed of 2° min^{-1}. Single-phase PZT powders obtained at 700 °C for $x = 0.515$, 0.520, 0.525 and 0.530 were sintered at 1000 °C for 2 h in a PbO atmosphere to increase the particle size for the detection of tetragonal/rhombohedral distortions in the XRD patterns. The weight of the pellet was taken before and after sintering to determine the PbO loss. It was confirmed that the weight loss is negligible (<0.1%). In order to compare the calcination temperature for the formation of single-phase PZT powders by the semi-wet route with that of those prepared by the conventional dry route, $PbCO_3$, ZrO_2 and TiO_2 were ball milled for 6 h for $x = 0.525$. This mixture was calcined at 700 °C for 6 h and the calcined powder was also X-rayed.

3. Results and discussion

3.1. Formation of $(Zr_xTi_{1-x})O_2$

The XRD pattern of the decomposed hydroxide for $x = 0.525$ is shown in Fig. 1. This XRD pattern is not of very good quality presumably due to the small particle size. All the lines in this pattern could, however, be indexed with respect to a tetragonal unit cell with $a = b = 0.5014$ nm and $c = 0.535$ nm. The calculated and observed d-spacings for the proposed tetragonal unit cell are found to be in good agreement, as shown in Table I. From this it can be concluded that the decomposed powder is a solid solution of ZrO_2 and TiO_2. The most intense line of TiO_2 for the anatase and rutile phases is not present in the XRD pattern. This further confirms that the titanium has replaced zirconium in the tetragonal modification of ZrO_2. The $(Zr_xTi_{1-x})O_2$ particles obtained are submicrometre in size (~0.2 μm) as can be seen from Fig. 2 which gives the scanning electron micrograph of the oxide powders. For pure ZrO_2, it is known [8] that the structure is tetragonal for particle sizes of less than 0.2 μm. Our work shows that the $(Zr_xTi_{1-x})O_2$ particles are also tetragonal up to about 0.2 μm.

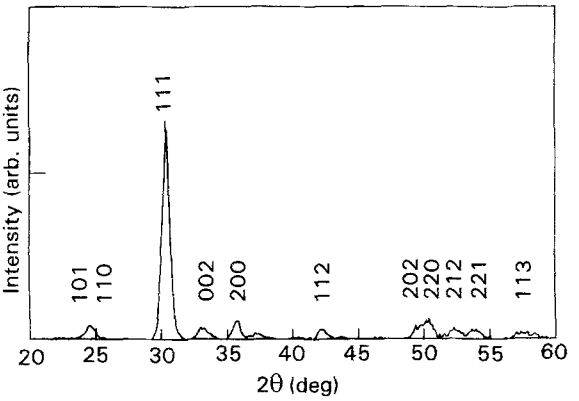

Figure 1 XRD pattern of $(Zr_{0.525}Ti_{0.475})O_2$ powders obtained after the decomposition of $Zr_{0.525}Ti_{0.475}(OH)_4$.

TABLE I Observed and calculated d-spacings for $(Zr_{0.525}Ti_{0.475})O_2$ powders obtained after the decomposition of $(Zr_{0.525}Ti_{0.475})(OH)_4$; all the lines have been indexed with respect to a tetragonal unit cell with $a = b = 0.5014$ nm and $c = 0.535$ nm

Indices	$2\theta_{obs}$ (deg)	d_{obs} nm	d_{cal} nm	I_{obs}
101	24.48	0.3633	0.3659	7
110	24.784	0.3589	0.3545	5
111	30.44	0.2934	0.2956	100
002	33.472	0.2675	0.2675	5
200	35.776	0.2507	0.2507	8
112	42.008	0.2149	0.2135	4
202	49.448	0.1841	0.1829	6
220	50.40	0.1809	0.1773	10
212	53.704	0.1747	0.1718	6
221	53.976	0.1697	0.1683	5
113	57.944	0.1590	0.1593	12

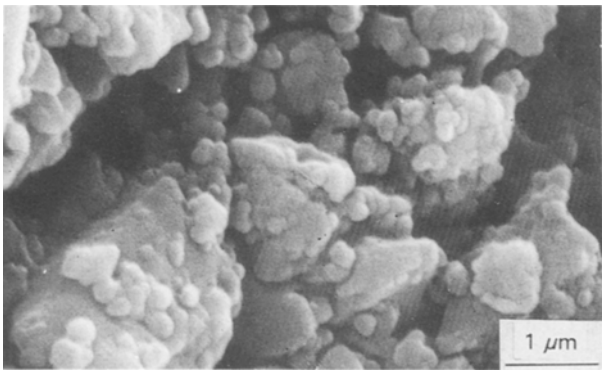

Figure 2 Scanning electron micrograph of $(Zr_{0.525}Ti_{0.475})O_2$ powders (36 kV).

It should be emphasized that the solid-solution character of $(Zr_xTi_{1-x})O_2$, obtained by the decomposition of $(Zr_xTi_{1-x})(OH)_4$, was not verified by Kakegawa *et al.* [2]. As a result of the solid-solution formation, the atomic-level homogeneity of Zirconium and Titanium is ensured in each precursor oxide particle irrespective of its size. This is in marked contrast to the typical micrometre-level separation of these ions in the particulate mixture of micrometre sized ZrO_2, TiO_2 and PbO particles for the conventional dry route of synthesis.

3.2. Optimization of PZT formation temperature

Fig. 3 depicts the DTA/TGA records for a mixture of $PbCO_3$ and $(Zr_{0.525}Ti_{0.475})O_2$ from room temperature up to 900 °C. It is evident that the weight loss occurs in three steps up to 440 °C after which there is no weight loss. Following Warne and Baylis [9], it is proposed that the three steps of the weight loss are due to the step-wise decomposition of $PbCO_3$ into PbO in the manner given below;

Step 1: $2PbCO_3 \longrightarrow PbO \cdot PbCO_3 + CO_2$
Step 2: $3(PbO \cdot PbCO_3) \longrightarrow 2(2PbO \cdot PbCO_3) + CO_2$
Step 3: $2PbO \cdot PbCO_3 \longrightarrow 3PbO + CO_2$

The theoretically expected weight losses of the mixture of $PbCO_3$ and $(Zr_{0.525}Ti_{0.475})O_2$ at each of the three steps are 6.9%, 8.8% and 11.9%. The observed percentage weight losses are 6.8%, 9.0% and 12.3% which are in very good agreement with the theoretically expected values for the three-step decomposition of $PbCO_3$. The broad exothermic peak running from nearly 430 to 700 °C in Fig. 3 appears to be due to the reaction of the PbO with $(Zr_{0.525}Ti_{0.475})O_2$. Accordingly, mixtures of $PbCO_3$ and $(Zr_{0.525}Ti_{0.475})O_2$ were calcined at 500, 600 and 700 °C to determine the PZT-formation temperature.

Fig. 4 gives the XRD pattern of the mixture calcined at 500 °C for 6 h; all the lines have been identified and are marked. The powder calcined at 500 °C essentially consists of PbO (litharge), TiO_2, $PbTiO_3$ and $(Zr_xTi_{1-x})O_2$. There is no trace of PZT lines at 500 °C. Calcination of the mixture of $PbCO_3$ with $(Zr_{0.525}Ti_{0.475})O_2$ at 600 °C for 6 h, on the other hand, yields powder which is single-phase PZT (see Fig. 5). The reaction is much faster at 700 °C since single-phase PZT powders could be synthesized within 2 h at this temperature, as is evident from the XRD pattern given in Fig. 6. From the foregoing, the temperature of formation of PZT by the semi-wet route is between 500 and 600 °C, which is quite low. From a comparison of the X-ray profiles given in Figs 5 and 6, it is

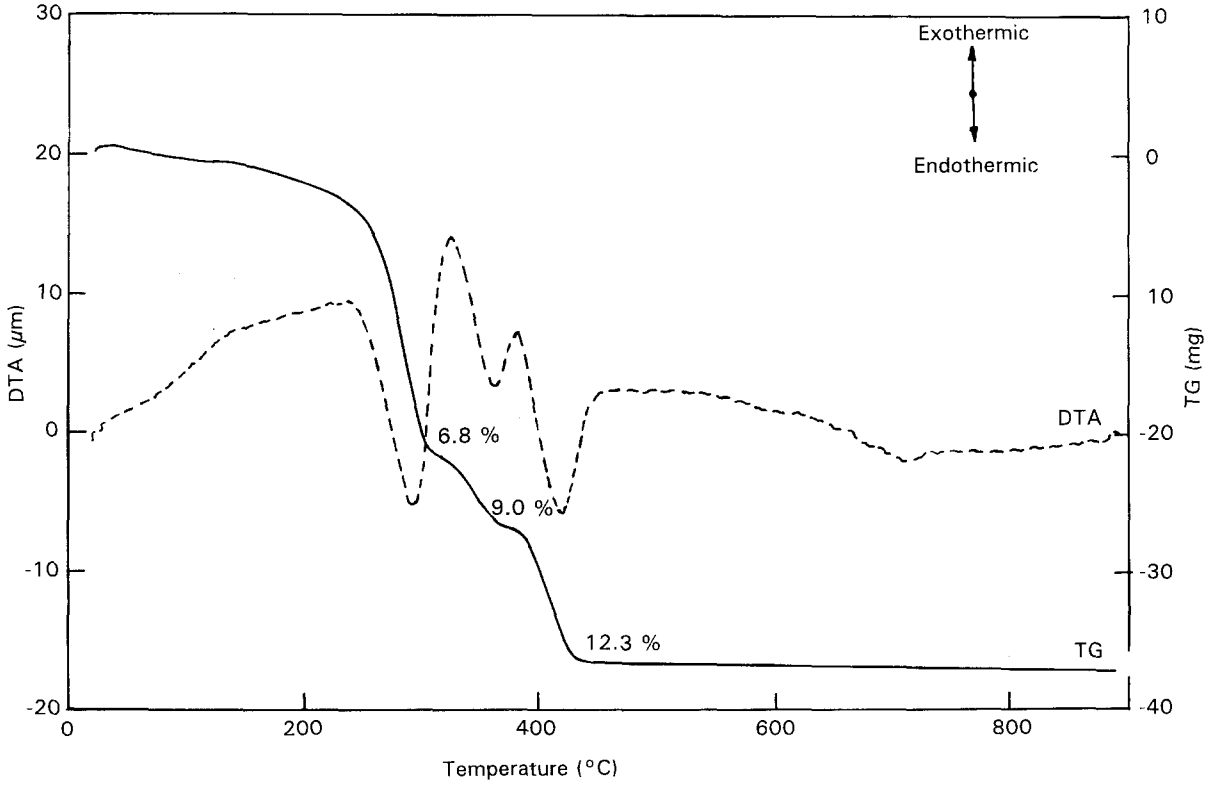

Figure 3 DTA/TGA of a mixture of $PbCO_3$ and $(Zr_{0.525}Ti_{0.475})O_2$: (—) TGA, and (- - -) DTA.

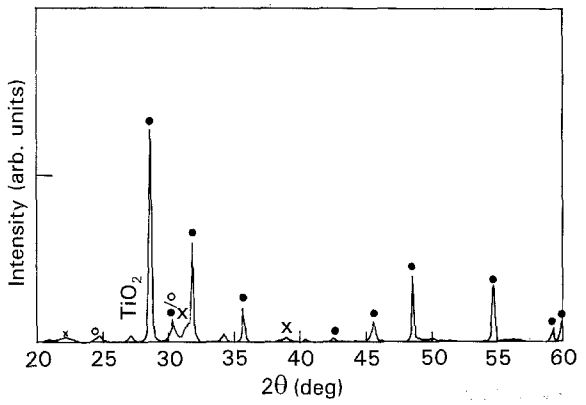

Figure 4 XRD pattern of the powder obtained after calcining a mixture of $PbCO_3$ and $(Zr_{0.525}Ti_{0.475})O_2$ at 500 °C for 6 h: (●) PbO, (○) $(Zr_{0.525}Ti_{0.475})O_2$, and (×) $PbTiO_3$.

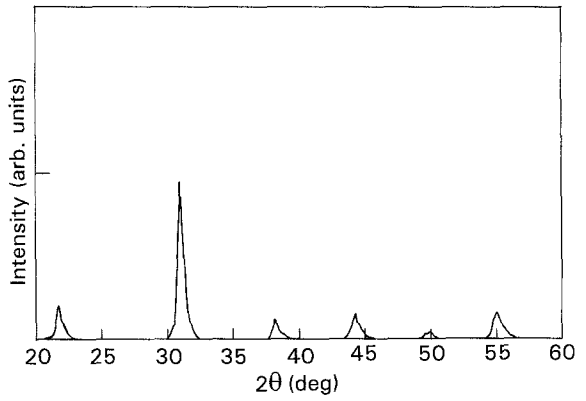

Figure 5 XRD pattern of the powder obtained after calcining a mixture of $PbCO_3$ and $(Zr_{0.525}Ti_{0.475})O_2$ at 600 °C for 6 h.

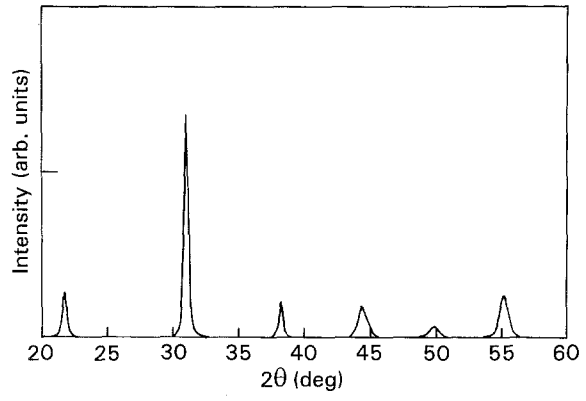

Figure 6 XRD pattern of the powder obtained after calcining a mixture of $PbCO_3$ and $(Zr_{0.525}Ti_{0.475})O_2$ at 700 °C for 2 h.

evident that reflections for powders calcined at 700 °C are sharper than for those calcined at 600 °C. This is due to the increase in the particle size of the PZT powders. As shown later, sintering of these powders at 1000 °C leads to further sharpening of the peaks due to grain growth during sintering.

It is worth mentioning that Kakegawa *et al.* [2, 7] used PbO in place of $PbCO_3$ in the semi-wet synthesis of PZT powders. It is found that the use of PbO in place of $PbCO_3$ in the semi-wet route raises the calcination temperature of formation of single-phase PZT powder. Fig. 7 depicts the XRD pattern of powders obtained after the calcination of PbO and $(Zr_{0.525}Ti_{0.475})O_2$ at 600 °C for 6 h. A comparison of Fig. 7 with Fig. 5 clearly reveals that the powder obtained is not a single-phase PZT but consists of a mixture of PbO, $(Zr_{0.525}Ti_{0.475})O_2$, PZT, and some unidentified phases. Thus, the lowering of the PZT formation temperature in our semi-wet route is not only due to the solid-solution precursor, $(Zr_{0.525}Ti_{0.475})O_2$, but also due to the use of $PbCO_3$ rather than PbO. It is expected that $PbCO_3$ particles on decomposition become finer PbO particles, which are nascent and surround the $(Zr_{0.525}Ti_{0.475})O_2$ precursor particles, before the formation of PZT begins. This contributes to the lowering of the PZT formation temperature.

For a comparison with the conventional dry route, a mixture of $PbCO_3$, $0.525ZrO_2$ and $0.475TiO_2$ was calcined at 700 °C. Even after 6 h of calcination of this mixture, there is no trace of PZT lines in the XRD pattern which is shown in Fig. 8. The calcined powder, so obtained, essentially consists of $PbTiO_3$, $PbZrO_3$ and unreacted PbO, TiO_2 and ZrO_2. Thus the semi-wet route for the synthesis of PZT powder is far superior to the conventional dry route since single-phase PZT powder can be prepared at as low a temperature as 600 °C.

The particle size of the calcined powders was determined by scanning electron microscopy (SEM) and X-ray line broadening. Fig. 9 gives the SEM micrograph

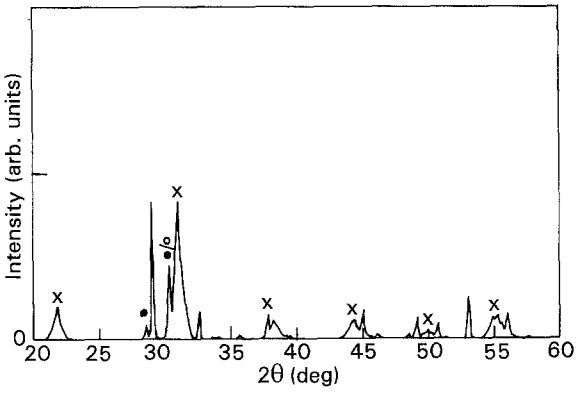

Figure 7 XRD pattern of the powder obtained after calcining a mixture of PbO and $(Zr_{0.525}Ti_{0.475})O_2$ at 600 °C for 6 h: (●) PbO, (○) $(Zr_{0.525}Ti_{0.475})O_2$, and (×) PZT.

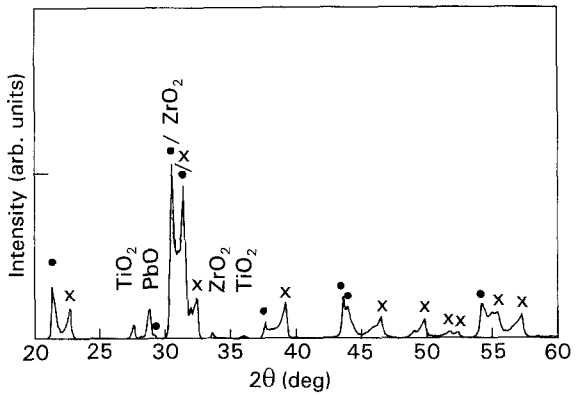

Figure 8 XRD pattern of the powder obtained after calcining a mixture of $PbCO_3$, ZrO_2 and TiO_2 at 700 °C for 6 h: (●) $PbZrO_3$, and (×) $PbTiO_3$.

of the powders calcined at 700 °C. It is evident that the powder is highly agglomerated. However, from the right-hand top of the micrograph, the average particle size can be assessed to be of the order of 0.1 μm. Calculation of the crystallite size from the 1 1 1 diffraction peak using the Scherrer formula, after removing instrumental broadening, gives a value of 50 nm. Both the measurements suggest that the powders are definitely of sub-micrometre size even though the individual values do not exactly match.

As mentioned in the introduction, use of solid-solution $(Zr_xTi_{1-x})O_2$ in place of ZrO_2 and TiO_2 not only reduces the diffusion distances involved during the formation of PZT but also favours direct formation of PZT by reactions between PbO and $(Zr_xTi_{1-x})O_2$ particles. In addition, since the number of nascent PbO particles obtained after the decomposition of $PbCO_3$ particles above 400 °C is considerable, each $(Zr_xTi_{1-x})O_2$ particle can be safely assumed to be in contact with PbO particles, thereby providing greater scope for faster reaction by reducing the diffusion distances. Further, PZT formation takes place by the diffusion of more mobile PbO into the refractory $(Zr_xTi_{1-x})O_2$ particles. All these factors are responsible for the formation of sub-micrometre sized PZT powders at a low temperature of 600 °C. In the conventional dry route of synthesis, initially $PbTiO_3$ is formed at lower temperatures followed by $PbZrO_3$ which then have to interdiffuse to yield PZT [1]. The kinetics of interdiffusion of $PbTiO_3$ and $PbZrO_3$ apparently requires much higher temperature than the diffusion of mobile PbO into $(Zr_xTi_{1-x})O_2$ in the semi-wet route. Apart from the higher calcination temperature for the formation of PZT by the conventional dry route, the powders are less reactive due to their bigger size. Further, there will be a lot of compositional fluctuations [2] at the Zr/Ti site in powders prepared by this route because of the long-range diffusion involved.

Figure 9 Scanning electron micrograph of PZT particles obtained after the calcination of a mixture of $PbCO_3$ and $(Zr_{0.525}Ti_{0.475})O_2$ at 700 °C for 2 h.

3.3. Location of the MPB

The XRD patterns of the as-calcined powders at 700 °C show pseudocubic character, irrespective of the Zirconium content, presumably due to the sub-micrometre particle size. On sintering these powders at higher temperatures in a PbO atmosphere (to prevent lead oxide loss), grain growth occurs and the tetragonal/rhombohedral distortions become discernible on X-ray diffractograms.

Fig. 10 depicts the X-ray diffractograms taken from sintered PZT powders for $x = 0.515$, 0.52, 0.525 and 0.53. Sintering was done at 1000 °C for 2 h in a PbO atmosphere. It is evident from Fig. 10 that the powder is single-phase tetragonal up to $x = 0.52$ while it is rhombohedral at $x = 0.53$ indicating the MPB to lie within $0.52 < x < 0.53$. However, for $x = 0.525$, both rhombohedral and tetragonal phases coexist, as can be inferred from the characteristic splittings of the $111/11\bar{1}$ and $200/002$ reflections in the zoomed profiles shown in the inset. As shown in the next section, this coexistence is not due to compositional fluctuations since the line-broadening analysis has shown that these powders are free from such fluctuations. The coexistence of tetragonal and rhombohedral phases has, therefore, to be attributed to the first-order nature of the MPB. This is in marked contrast to the proposition of Kakegawa *et al.* [2, 7] that the coexistence is invariably due to compositional fluctuations. The intrinsic range of composition for this coexistence is, however, very narrow ($\lesssim 0.01$) and is easily distinguishable from the extrinsic, wide ($\Delta x \sim 0.15$) range of coexistence region in compositionally inhomogeneous samples prepared by the conventional dry route [10].

3.4. Compositional homogeneity analysis

For the compositional homogeneity analysis, samples were chosen which were sintered at 1000 °C with $x = 0.515$ and 0.53 (tetragonal and rhombohedral, respectively). In order to obtain the true diffraction broadening from the measured profiles, the $K\alpha_2$ contribution was first removed using Rachinger's method [11]. The effect of instrumental broadening was removed using a Silicon standard specimen in a manner described in detail elsewhere [11]. Graphs of $\beta\cos\theta$ versus $\sin\theta$, where β is the halfwidth of the true diffraction profile and θ is the Bragg angle, are shown in Fig. 11 for $x = 0.515$ and 0.530. The horizontality of the least-squares fitted lines to the data points in the two figures confirms [2, 11] that there is no fluctuation in d-spacings due to compositional fluctuations at the Zr/Ti site. Thus the powders prepared using the heat-treatment protocol described in the present work

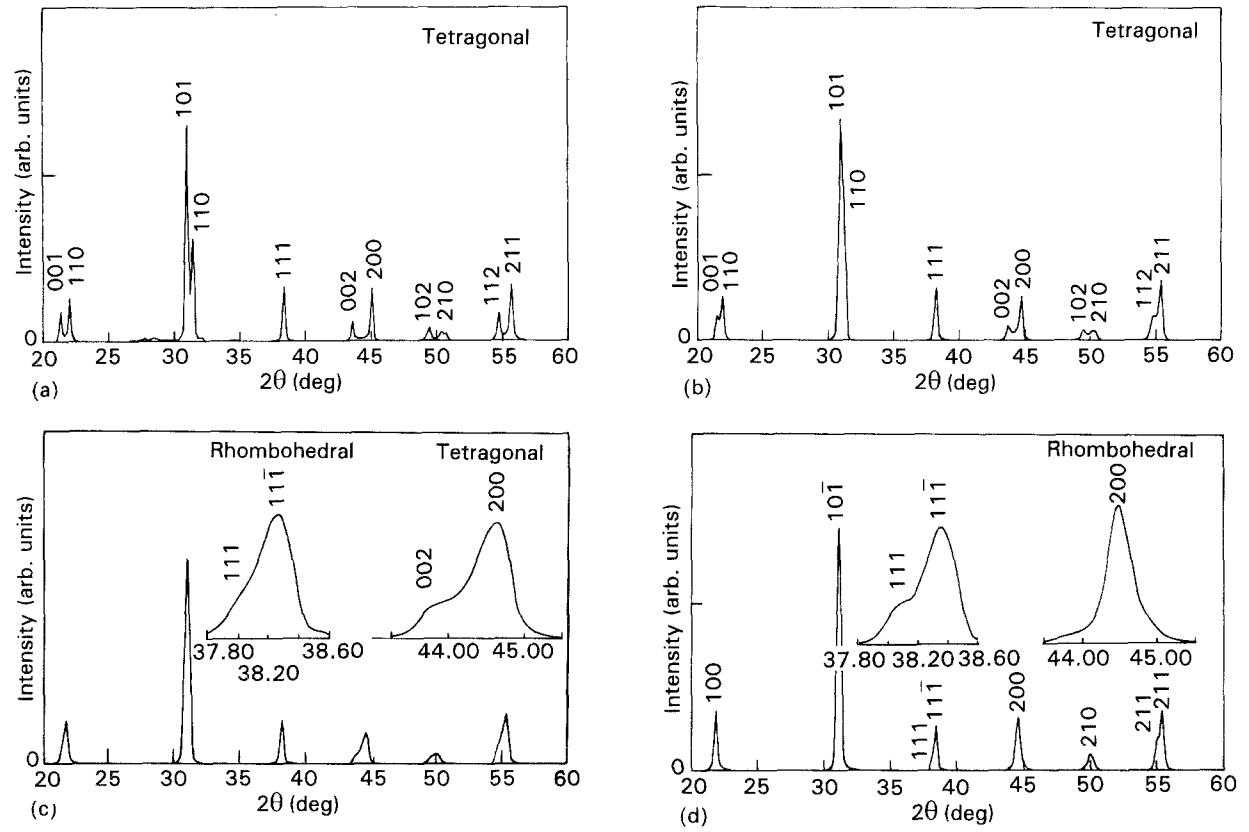

Figure 10 XRD patterns of $Pb(Zr_xTi_{1-x})O_3$ powders obtained after crushing the pellets sintered at 1000 °C for 2 h: (a) $x = 0.515$, (b) $x = 0.520$, (c) $x = 0.525$, and (d) $x = 0.530$. Note the coexistence of tetragonal and rhombohedral splittings in the inset to (c).

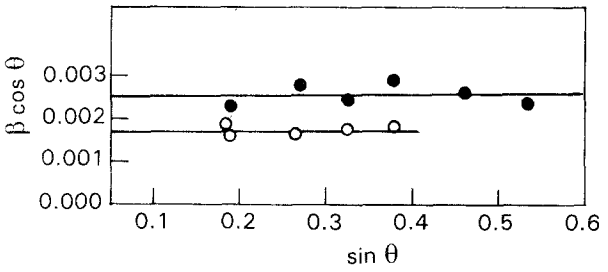

Figure 11 Plots of $\beta \cos\theta$ versus $\sin\theta$ for (○) $Pb(Zr_{0.515}Ti_{0.485})O_3$ and (●) $Pb(Zr_{0.530}Ti_{0.470})O_3$ powders obtained after crushing the pellets sintered at 1000 °C for 2 h. The continuous line is the best fit to the data points. The errors in the data points are much less than the size of the circles.

are compositionally homogeneous and yet show coexistence of rhombohedral and tetragonal phases over an extremely narrow range of composition ($\Delta x \lesssim 0.01$).

4. Conclusions

1. It was shown that $(Zr_xTi_{1-x})O_2$ solid solutions for $x = 0.515$ to 0.53 can be formed by thermal decomposition of coprecipitated $(Zr_xTi_{1-x})(OH)_4$.

2. Single-phase sub-micrometre sized PZT powders can be formed at 600 °C by the diffusion of mobile PbO into refractory $(Zr_xTi_{1-x})O_2$ on calcining a mixture of $PbCO_3$ with $(Zr_xTi_{1-x})O_2$.

3. The PZT powders prepared by the semi-wet route are compositionally homogeneous.

4. The MPB lies between $0.52 < x < 0.53$. For $x = 0.525$, there is a coexistence of tetragonal and rhombohedral phases even in compositionally homogeneous PZT powders.

Acknowledgements

We are grateful to Dr R. Krishnan and Dr P. C. Deb, past and present Directors of the Naval Chemical and Metallurgical Laboratory, Bombay, for their constant encouragement. Financial assistance from the Defence Research and Development Organization for this work is also gratefully acknowledged.

References

1. B. JAFFE, W. R. COOK and H. JAFFE, "Piezoelectric ceramics", (Academic Press, London, 1971).
2. K. KAKEGAWA, J. MOHRI, K. TAKAHASHI, H. YAMAMURA and S. SHIRASHAKI, *Solid State Commun.* **24** (1977) 769.
3. B. V. HIREMATH, A. I. KINGON and J. V. BIGGERS, *J. Amer. Ceram. Soc.* **66** (1983) 790.
4. V. S. TIWARI, D. PANDEY and P. GROVES, *J. Phys. D* **22** (1989) 837.
5. D. PANDEY, V. S. TIWARI, A. K. SINGH and S. CHAUDHRY, *Bull. Mater. Sci.* **12** (1989) 245.
6. D. PANDEY, R. MAHESH, A. K. SINGH, V. S. TIWARI and S. K. KAK, *Physica C* **184** (1991) 165.
7. K. KAKEGAWA, J. MOHRI, S. SHIRASAKI and K. TAKAHASHI, *J. Amer. Ceram. Soc.* **65** (1982) 515.
8. R. DAYAL, N. M. GOKHALE, S. C. SHARMA, R. LAL and R. KRISHNAN, *Brit. Ceram. Trans. J.* **91** (1992) 45.
9. S. St. J. WARNES and P. BAYLISS, *Amer. Miner.* **47** (1962) 1011.
10. W. A. RACHINGER, *J. Sci. Instrum.* **25** (1948) 254.
11. D. PANDEY, V. S. TIWARI and A. K. SINGH, *J. Phys. D.* **22** (1989) 182.
12. P. ARI-GUR and L. BENGUIGUI, *J. Phys. D* **8** (1975) 1856.

Received 7 July 1992
and accepted 3 February 1993